

SUPPORTING INFORMATION

S1. Temperature measurements in lab-scale experiments

Temperature measurements were recorded with 4-wire PT100 sensors using an Adafruit PT100 RTD Temperature Sensor Amplifier - MAX31865 connected to Arduino Nano boards. PT100 sensors were calibrated by setting constant temperatures in the water bath, within the temperature range expected to be used in the lab-scale tests (20-35°C). For this purpose, resistance and temperature values were measured once each water temperature was stabilized in the water bath. Resistance Temperature Detector (RTD) measurements were compared and adjusted with the data collected from one of the PT100 sensors, which was taken as a reference. After calibrating the RTD measurements, the Callendar-van Dusen (CvD) formula was applied to transform the RTD to temperature values (REF):

$$RTD = R_0 \cdot (1 + A \cdot T + B \cdot T^2), \text{ if } T > 0 \quad (S1)$$

where T is the temperature (°C), R_0 is the resistance at 0°C and its value is equal to 100 ohms, and $A = 3.9083E-03$ and $B = -5.775E-07$ are the coefficients of the CvD formula. This formula accurately approximates the relationship between resistance and temperature, with a maximum error of 0.0022°C within a temperature range of 0 to 200 °C.¹

S2. Thermal properties and leakage coefficient references

To improve convergence of the minimization algorithm within the cross-validation process, the ranges of sediment thermal properties and leakage heat loss coefficient were constrained. For this purpose, reference values were obtained from Hamdham and Clarke (2010) and Koju (2017),^{2,3} respectively. Thermal properties are combined in terms of the thermal diffusivity $k_e = k/\rho c_p$, while the leakage coefficient is defined as $\alpha = h/k$, where k is the thermal conductivity (W/m°C), ρ is the bulk density (kg/m³), c_p is the specific heat capacity (J/kg°C), and h is the convective heat transfer coefficient (W/m²°C).

Bulk density was measured in the laboratory ($\rho = 1625 \pm 7$ kg/m³), however, k and c_p values were estimated from references (Table S1). The convective heat transfer coefficient in expanded polystyrene (EPS) boxes was assumed to be $h = 2.06$ W/m²°C at ambient temperature.³ Therefore, thermal diffusivity (k_e) was constraint between 0.37 – 1.21 m²/s, and the leakage heat loss of the boxes to $\alpha \geq 0$. Leakage coefficients close to zero imply a high box isolation. Furthermore, all adiabatic boxes were assumed to have the same leakage coefficient.

Table S1. Reference values of sediment thermal properties. Adapted from Hamdham and Clarke (2010).²

Saturated soil type	Bulk density, ρ kg/m^3	Thermal conductivity, k $W/m^{\circ}C$	Specific heat capacity, c_p $J/kg^{\circ}C$	Thermal diffusivity, k_e m^2/s
Clay	1730	1.52	2362	0.37×10^{-6}
Fine Sand	2010	2.75	1632	0.84×10^{-6}
Medium Sand	2080	3.34	1483	1.08×10^{-6}
Coarse Sand	2080	3.72	1483	1.21×10^{-6}

S3. Numerical simulation of laboratory experiments

Figure S1 includes sediment-bed temperature timeseries simulated by applying the average k_e and α values from cross-validation process (section 3.1.3), and the performance assessment compared to lab-scale measurements. The performance assessment between experimental and simulated sediment-bed temperature series was evaluated using the Nash-Sutcliffe model efficiency coefficient (NSE). In general, NSE coefficients were significantly high with an average score of 0.91. A better model performance was observed for tests with higher thicknesses, while largest discrepancies were obtained for the model with the lowest thickness ($H_{sed} = 2$ cm).

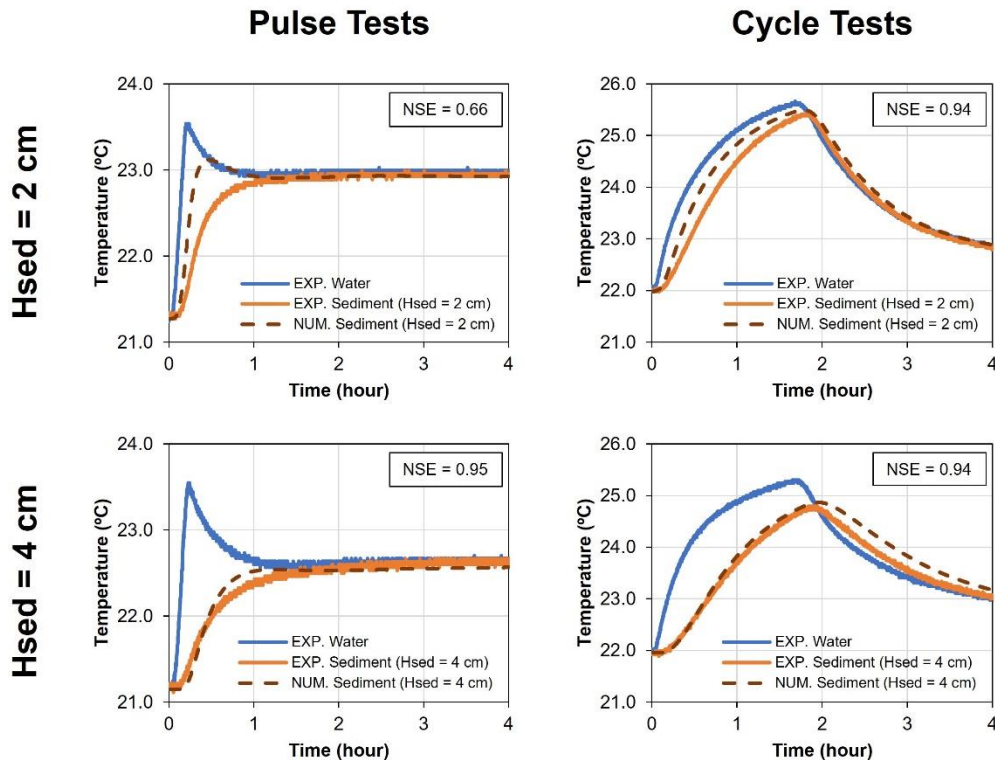


Figure S1. cont.

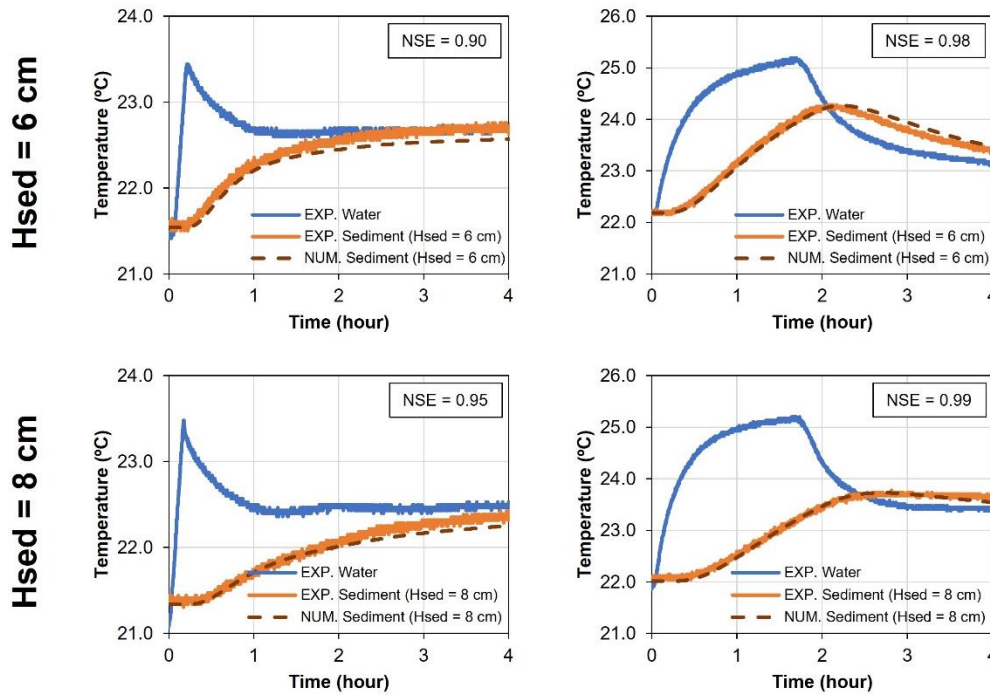


Figure S1. Heat-pulse (top row) and cycle (bottom row) lab-scale tests: experimental and numerical comparison. Experimental water (blue line) and sediment-bed (orange line) temperatures, and best-fit simulated sediment-bed temperatures (dashed brown line).

S4. Synthetic sediment-bed temperatures

Due to the lack of references of temperatures conditioned by sewer sediment deposits, synthetic sediment-bed temperatures were simulated by applying the calibrated 1D heat transfer model. For this purpose, wastewater temperature time series from Eawag's Urban Water Observatory (Fehraltorf, Switzerland) were introduced as top boundary conditions in the numerical model.⁴ To obtain close-to-real temperature time series, initial conditions in sediment-bed temperatures were obtained by warming up the 1D heat transfer model. Several initial temperatures were analyzed by adding a gradient to the initial wastewater temperature $[0, \pm 0.25, \pm 0.50]$ °C. Figure S2 shows that simulations converge after 24 hours for a sediment thickness of 15 cm under both dry weather time series collected from UWO (DW1 and DW2). Therefore, 1-day warming-up of the model was established to ensure suitable initial sediment-bed temperature conditions in the simulations.

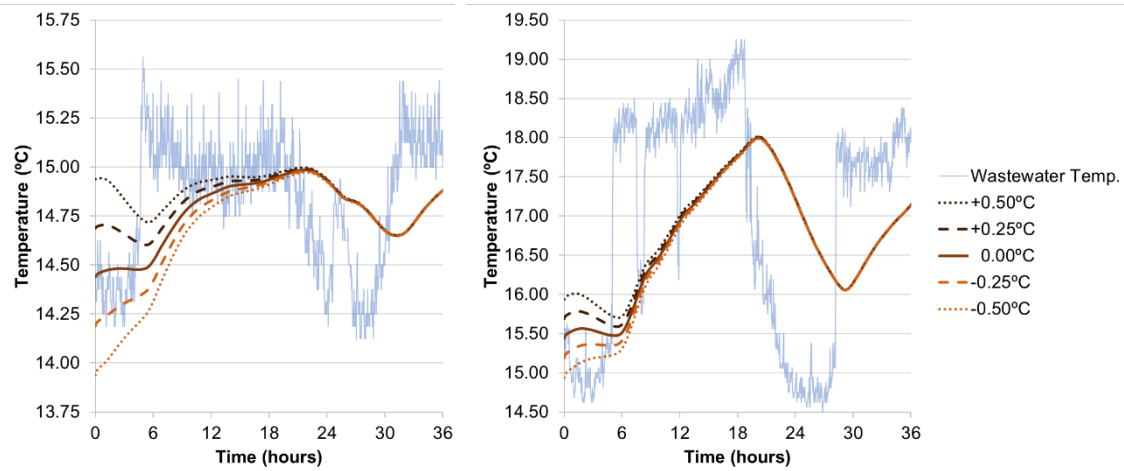


Figure S2. Synthetic sediment temperature simulated with different initial conditions from the initial wastewater temperature $T_{w|t=0}$ [-0.50; -0.25; 0; +0.25; +0.50]. Results plotted were obtained for $H_{sed} = 15$ cm, 1.5 days of simulation and dry weather boundary conditions (DW1, left; DW2, right).

Furthermore, normal random noise signal ($\sigma = 0.1^\circ\text{C}$) was introduced to approach realistic measurements in sewers, as sediment-bed temperature simulations do not consider spontaneous temperature and sensor artifacts. Figure S3 shows time intervals of sediment-bed temperatures obtained by applying the 1D heat transfer model for a sediment thickness of 15 cm under both dry weather time series collected from UWO (DW1 and DW2), and the implementation of the random noise signal.

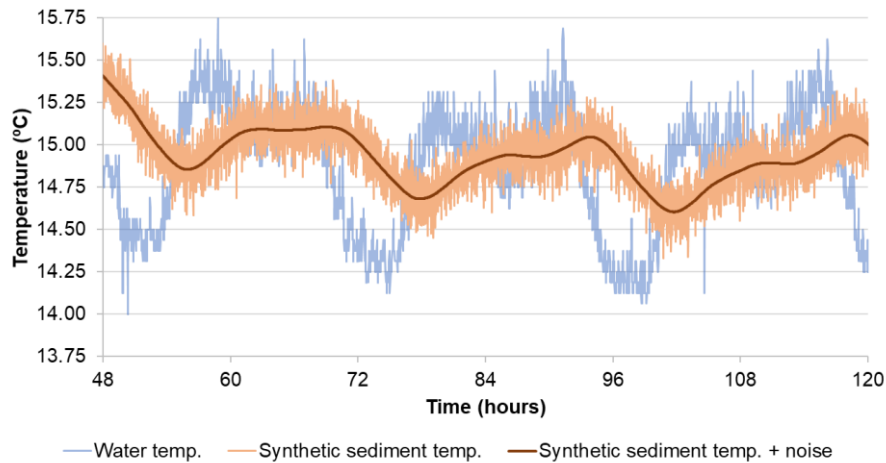


Figure S3. Cont.

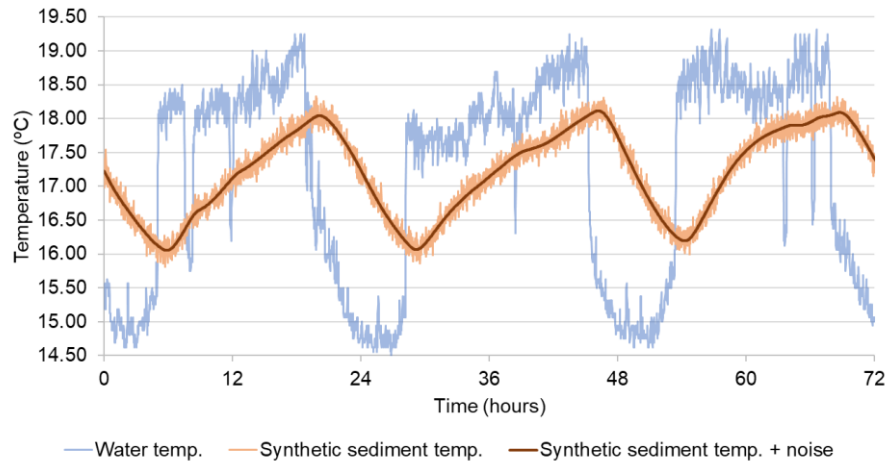


Figure S3. Wastewater temperature measurements (blue line) and simulated sediment-bed temperatures (brown line), including random noise signal implementation (orange line). Note that this plotted was obtained by simulating a sediment thickness of $H_{sed} = 15\text{cm}$, and dry weather boundary conditions ($DW1$, top; $DW2$, bottom).

S5. Significance of the period of temperatures analyzed

Sediment accumulation processes show continuous dynamics, although daily sediment accumulation rates are low under dry weather conditions.⁵ The methodology presented in the main document considers a constant sediment-bed throughout the temperature time series. Therefore, this section discusses the importance of the preceding time considered for the sediment thickness estimation. Figure S4 shows the sediment height estimation error based on the Dynamic Harmonic Regression (DHR) method as a function of the total period of temperature measurements analyzed under dry weather conditions. We observed that at least a 2-day period in the temperature timeseries should be analyzed to obtain an estimation error less than 10% under constant sediment thickness conditions. This error becomes smaller as the volume of deposited sediment increases. Considering the accumulation rates in sewer pipes (0.8 and 6.2 mm/day, following Regueiro-Picallo *et al.*, 2020)⁵, this period is acceptable for accurate sediment height estimations under dry weather conditions. Regarding wet weather periods, a high uncertainty in the estimation will have to be assumed due to possible high erosion rates under these conditions.

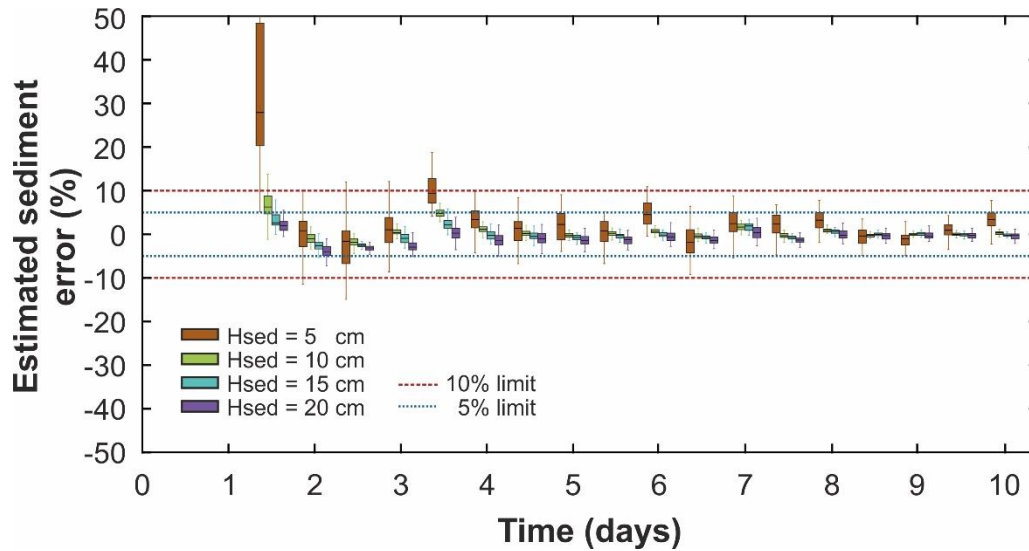


Figure S4. Sediment height estimation errors based on the time-period of temperature timeseries under dry weather conditions analyzed by applying DHR method. Note that only sediment heights of 5, 10, 15, and 20 cm are included. Pointed and dashed lines represent errors of 5% and 10%, respectively.

S6. References

1. G. King, T. Fukushima, in *RTD Interfacing and Linearization Using an ADuC8xx MicroConverter®. AN709, Analog Devices.*, 2004.
2. I. N. Hamdhan, B. G. Clarke, presented in part at World Geothermal Congress, Bali, Indonesia, April, 2010.
3. S. M. Koju, *J. Sci. Eng.*, 2017, **4**, 47-52.
4. The Urban Water Observatory - Long-term monitoring of urban water resources dynamics in very high spatiotemporal resolution using low-power sensor and data communication techniques, <https://uwo-opendata.eawag.ch/>, (accessed 16 August 2022).
5. M. Regueiro-Picallo, J. Suárez, E. Sañudo, J. Puertas, J. Anta, *Sci. Total Environ.*, 2020, **716**, 136923.